Biotechnology and Bioprocess Engineering
DOI 10.1007/s12257-021-0243-6

pISSN 1226-8372
eISSN 1976-3816

RESEARCH PAPER

Crosslinker-free Bovine Serum Albumin-loaded Chitosan/alginate Nanocomplex for pH-responsive Bursting Release of Oral-administered Protein

Jiaoyang Li, Hui Jin, Md. Abdur Razzak, Eun Ji Kim, and Shin Sik Choi

Received: 27 August 2021 / Revised: 19 October 2021 / Accepted: 22 October 2021

Abstract The application of protein-based drugs in oral delivery system is limited due to the harsh environment of the gastrointestinal (GI) tract. Herein, a pH-responsive nano-sized complex with chitosan (CH) and alginate (AL) was fabricated without cross-linker as an oral vehicle for bursting release of protein at the target location to enhance the efficacy. Using bovine serum albumin (BSA) as a model cargo protein, four optimized complexation processes (LG1, LG2, LG3, and LG4) were selected by changes of variables (total concentration (TC), the ratio of CH to AL (CH/AL, w/w), and mixing time (MT)) and further modifications using encapsulation efficiency and complex size. Size, ζ-potential, morphology, BSA release, and swelling degrees of the complexes were evaluated under simulated gastrointestinal conditions (pH 2.0 and 7.4). LG1 and LG4 completely retained BSA in complexes at pH 2.0 after 2 h (BSA release percentage is 0%) and exhibited bursting release at pH 7.4 after 1 h (84.03 and 67.59%, respectively). Low absolute ζ-potential value (about 10 mV), large size (over 10000 nm) and polymer morphology demonstrated that the pH-responsive complexes inhibited protein release at pH 2.0 through the molecule-molecule aggregation. Relatively high absolute ζ-potential value (about 45 mV), ideal swelling ability (around 2), and polymer morphology revealed that the complex promoted the release at 7.4 through both micro- and macroscale swelling. Results demonstrate that the CH-BSA-AL complex through LG4 has a potential for administering protein-based drugs or vaccines orally due to its highest effective dose (78.78 μg/mL).

Keywords: low molecular chitosan, alginate, complex, bursting release, degree of swelling

Jiaoyang Li, Md. Abdur Razzak, Shin Sik Choi*
Department of Energy Science and Technology, Myongji University, Yongin 17058, Korea
Tel: +82-31-330-6478; Fax: +82-31-330-6200
E-mail: sschoi@mju.ac.kr

Hui Jin
Center for Nutraceutical and Pharmaceutical, Myongji University, Yongin 17058, Korea

Eun Ji Kim, Shin Sik Choi
Department of Food and Nutrition, Myongji University, Yongin 17058, Korea

Shin Sik Choi
Natural Science Research Institute, Myongji University, Yongin 17058, Korea

1. Introduction

The protein-based drugs play an important role in the pharmaceutical industry, especially in novel therapies. The U.S Food and Drug Administration (FDA) center has approved 239 therapeutic peptides and proteins [1]. The main classes include monoclonal antibodies, coagulation factors, replacement enzymes, fusion proteins, hormones, growth factors, and plasma proteins. These proteins are applied to a wide variety of therapeutic areas, such as cancers, cardiovascular diseases, genetic disorders, inflammation, infectious, and metabolic diseases, *etc*. [2]. In practical applications, a large proportion of protein-based drugs are administered parenterally (intravenous, subcutaneous, or intramuscular injections) because of highly bioavailable [3]. However, its poor compliance [4,5], severe issues at the injection site (allergic reaction [6] and cutaneous infections [7]), requirements for professional administration [8] limits its widespread use.

Oral delivery systems have received significant attentions because of their low costs, easy administration, effective

mucosal immunities, and low professional requirements [9,10]. Although oral delivery systems have been well used for small molecule drugs, the biopharmaceuticals with large molecular weight of protein or peptide medicines have been rarely chosen. The bioavailability of protein-based drugs via oral administration was very low (0.1-1%) due to the harsh gastrointestinal tract [11,12]. Since proteins are easily denatured or unfolded upon deviating from neutral pH, the strong acid stomach condition (pH 1.0-2.0) readily causes proteolytic breakdown before proteins reach a circulation system through the small intestine (pH 7.4) [13]. It is therefore necessary to develop drug delivery systems to protect oral administration of protein-based drugs. Micro-and nanoparticles have been studied extensively as delivery carriers for protein-based drugs such as virus-like particles loaded with HPV [14], HIV [15], and H1N1 [16]; liposomes (non-viral lipids) of loading circumsporozoite (malaria) [17] and CtUBE fusion peptide [18]; polymeric particle of loading docetaxel and hepatitis B [19,20]. It is considered advantageous to include natural hydrophilic polycolloids in the design of wall materials because of their biocompatibilities, biodegradability, and good drug-loading capacities [21].

Chitosan (CH) is a cationic linear polymeric polysaccharide containing an amino group, which is mainly found in fungi, molluscs, and insects. CH has been considered as a competent carrier of oral protein drugs because of biocompatible [22], biodegradable [22], and muco-adhesiveness in specific regions [23-25]. The pH sensitivity of CH that is easily soluble at acidic pH, whereas insoluble in neutral pH is provided by the large number of amino groups on its chain, which is responsible for effective gastric drug delivery [26]. However, this property is limited to the intestinal drug delivery because the CH-loaded protein is denatured as the CH matrix dissolves under acidic conditions. Alginate (AL) is a water-soluble linear polysaccharide composed of α-L-guluronic (G-block) and β-D-mannuronic (M-block) acid residues [26]. The structure and molecular weight of AL provide the physical properties of biocompatibility [27] and bio-adhesiveness [28]. The pH sensitivity of AL that shrinks under acidic pH, whereas swells at neutral [29] is the main advantage as an oral drug delivery system. However, the AL-entrapped protein may be denatured because of the proteolytic enzymes that result in rapid dissolution of AL in an alkaline environment. The complementary biological characteristics of CH and AL makes their combined use widespread in oral delivery systems [30-33]. Bovine serum albumin (BSA) has been widely used as a model protein in the research of protein drug delivery systems owing to its high purity, water-solubility, and low cost [34-37].

Studies on BSA-loaded CH/AL complexes have almost entirely dedicated to slowing the release with approximately 25% of BSA release after 12 h at pH 7.4 [38], also controlling release with up to ten days of low BSA percentage [39] for minimizing undesirable side effects. However, when the host is non-human, such as poultry, the drug was allowed to remain in the gastric tract for 2 h [35] and the small intestinal tract for 4 h [40]. The oral delivery system described above apparently causes the drug to be eliminated from the host before release from complex. However, research on the fabrication of CH/AL complexes with bursting release in the small intestine have rarely been reported.

In this study, we fabricated nanometer-sized biocompatible polysaccharide complexes through the optimized molecule-molecule complexation process and investigated their physicochemical characterization, encapsulation efficiency, pH-responsible and swelling degree. This study presents a promising oral delivery system with bursting release of protein-based drugs or vaccines using BSA as a model protein cargo encapsulated through the complexation with CH and AL.

2. Materials and Methods

2.1. Materials

BSA (water-soluble, 40 mg/mL), CH (molecular weight 90~150 kDa), low molecular chitosan (molecular weight 40~50 kDa), AL from brown algae, NaH_2PO_4, Na_2HPO_4, and KCl were purchased from Sigma-Aldrich, USA. Acetic acid (99.5%) and HCl (35.0-37.0%) were purchased from Samchun Chemical, Korea. All chemicals were of analytical grade.

2.2. Experimental design

An orthogonal test of three factors and three levels with encapsulation efficiency (EE) and size as response values was designed to evaluate the effect of total concentration (TC), ratio of CH to AL (w/w), and mixing time (MT) on the formation of the complexes. The coded form of the design matrix is summarized in Table 1. MT indicates the time to continue stirring after each component has been mixed. The MT of the G1, 0 h means that the preparation was immediately terminated as soon as each component (CH, BSA, and AL) was mixed without further agitation.

Table 1. Factors and levels implemented for CH-BSA-AL complex formation

Factors Levels	TC (%)	CH/AL (w/w)	MT (h)
1	0.08	20:80	0
2	0.4	40:60	6
3	0.8	70:30	12

2.3. Preparation of CH-BSA-AL complexes

First, CH and AL were dissolved in acetic acid (20 mM) and distilled water, respectively. Thereafter, their solutions were shaken overnight at room temperature to obtain fully dissolved solution stocks. BSA was dissolved in distilled water to obtain a 100 μg/mL solution. Next, 2 mL of the BSA solution was added dropwise into 9 mL of the AL solution at a rate of 0.07 mL/min with continuous stirring (300-350 rpm). Thereafter, the complex mixture (BSA-AL) was added dropwise into CH solution at a rate of 0.33 mL/min with continuous stirring (300-350 rpm). The height of the syringe from the bottom of the beaker was approximately 15 cm. The resulting solution was centrifuged at 4,500 rpm for 20 min at 25°C, and then the supernatant was discarded. Thereafter the pellet was dried in an oven (60°C) approximately 2 h to remove the residual solvent on the surface (Fig. 1). The resulting substance was the CH-BSA-AL complex that was used in this study.

2.4. Determination of BSA encapsulation efficiency (EE)

One milliliter of CH-BSA-AL complex solution was centrifuged (15,000 rpm, 20 min, 4°C) before drying. The EE was determined indirectly by measuring the free BSA concentration in the supernatant. The BSA concentration was measured using a Pierce BCA protein assay kit [41] (Thermo Fisher Scientific Co. Ltd., USA). First, 25 μL of a supernatant was added to 200 μL working reagents solution (Reagent A contained sodium carbonate, sodium bicarbonate, bicinchoninic acid, and sodium tartrate in 0.1 M sodium hydroxide. Reagent B contained BSA at 2 mg/mL in 0.9% saline and 0.05% sodium azide) and incubated at 60°C for 30 min. Afterward, absorbance was detected at 562 nm using a microplate reader. The concentration of BSA in supernatant was calculated using a standard curve. The formula for calculating the EE is as follow:

$$\text{EE}\,(\%) = \frac{\text{Total concentration of BSA (100 μg/mL)} - \text{BSA concentration in supernatant}}{\text{Total concentration of BSA (100 μg/mL)}} \times 100 \quad (1)$$

2.5. Determination of the characteristics of CH-BSA-AL complex

Physicochemical characterization of CH-BSA-AL nano-complexes was based on their size, polymer disperse index (PDI), and ζ-potential. These properties were determined using a Zetasizer Nano ZS (Malvern Panalytical Co. Ltd., USA) that utilizes dynamic light scattering (DLS). All measurements were performed at the refractive index of 1.330 (25°C). Each sample was tested at least three times. The morphologies of the complexes were observed by scanning electron microscopy (SEM). The complex solution was poured on a cover slide (2 × 2 cm^2) and placed in an oven (70°C) to dry completely before observation. The morphology was observed under the Hitachi SU8010 SEM (Hitachi, Co. Ltd., Japan) operated at 5.0 kV.

2.6. BSA release

We investigated the BSA release in the simulated GI conditions (pH 2.0 and pH 7.4) according to the following procedures (Fig. S1). First, the dried complex was resuspended in a HCl-KCl buffer (20 mM, pH 2.0) and incubated in a shaking incubator (220 rpm, 37°C) for 2 h. Thereafter, the solution was centrifuged (4500 rpm, 20 min), and then the pellet was resuspended in a phosphate buffer solution (PBS) (20 mM, pH 7.4) for 4 h. At the indicated

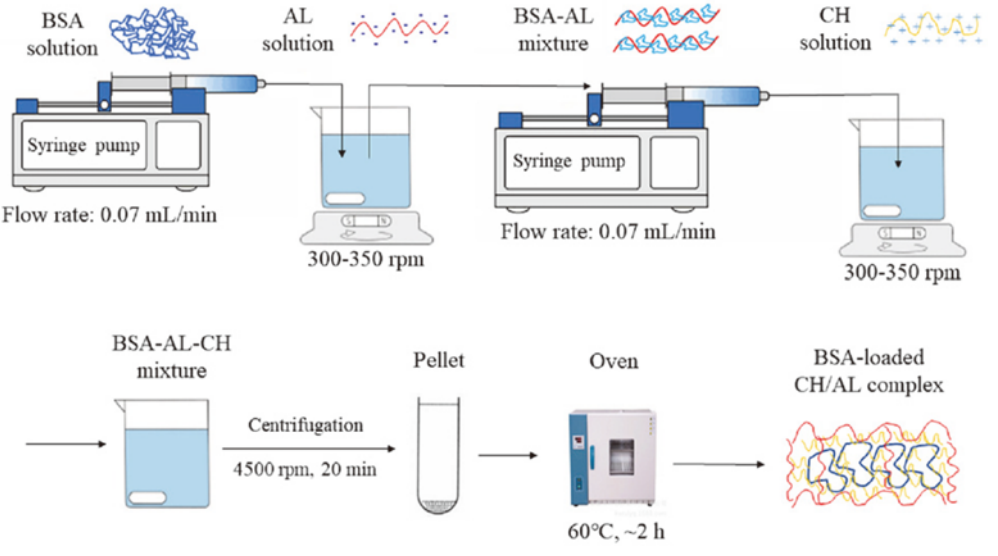

Fig. 1. The schematic process of CH-BSA-AL complex fabrication. BSA: bovine serum albumin. AL: alginate. CH: chitosan.

time points, after the centrifugation of the resuspended pellet at 15,000 rpm for 15 min, the released BSA concentration in the supernatant was determined by BCA assay using a microplate reader at 562 nm through the following calculation formula:

$$\text{Release percentage (\%)} = \frac{\text{BSA concentration in the supernatant}}{\text{Concentration of the encapsulated BSA (EE)}} \times 100 \quad (2)$$

2.7. Determination of degree of swelling (DS) of CH-BSA-AL complexes

The method from Tapia *et al*. was used as a reference with some modification [39]. First, the CH-BSA-AL complex solution was lyophilized. Thereafter, the powder was pressed using an infrared (IR) tablet press (15 Ton Hydraulic KBr Press, PerkinElmer, Co. Ltd., USA) to obtain tablets with a diameter of 1 ± 0.05 cm and a thickness of 0.3 ± 0.05 cm. Afterward, the tablets were immersed in pH 2.0 buffer (HCl-KCl, 20 mM) and pH 7.4 buffer (PBS, 20 mM). Images were obtained at specific time points (every 5 min for 125 min), and the areas of the tablets was measured using Image J. The monitoring endpoint was set at 125 min because the morphologies of the tablets did not change significantly after 125 min. *DS* of complex in pH 2.0 and pH 7.4 and the ratio of *DS* were expressed using formulas (3) ~ (5):

$$DS \text{ in pH } 2.0 = \frac{\text{Area of swollen tablet in pH 2.0 buffer}}{\text{Area of dried tablet}} \quad (3)$$

$$DS \text{ in pH } 7.4 = \frac{\text{Area of swollen tablet in pH 7.4 buffer}}{\text{Area of dried tablet}} \quad (4)$$

$$\text{The ration of } DS = \frac{DS \text{ in pH } 7.4}{DS \text{ in pH } 2.0} \quad (5)$$

3. Results and Discussion

3.1. Encapsulation of bovine serum albumin (BSA) with alginate (AL) and chitosan (CH)

For the CH-BSA-AL complexes, the effects of the concentrations of CH and AL [38,40] and BSA loading content [42,43] on the formation of a complex were studied. However, no relevant studies have been established on the embedding order and mixing time for the complex formation. In this study, an orthogonal test (three factors and three levels) was carried out to investigate the effect of total concentration (TC), the ratio of CH to AL (CH/AL (w/w)), and mixing time (MT) on encapsulation efficiency (EE) and complex size (Table 2). The smaller complex size implies the higher physicochemical stability and biocompatibility [44]. The smallest size was obtained in the group 1 (329.13 nm) with undesirable EE (45.66%). The highest EE (98.81%) was obtained in the group 6 with large size (5,752 nm). To screen the optimized condition for the formation of complex (high EE and small size), a variance analysis was carried out based on the EE and size of nine groups. Results showed that the most influential factor for EE and size were MT and TC, respectively (Table S1 and S2). The results from Sevgi *et al*. [38] also indicated that the concentration of wall materials had a significant effect on the particle size of the CH/AL beads (p = 0.0167).

To select the best level for each factor, the range analysis, a statistical method of showing the sensitivity and optimal value of the factor to specific results by the distance between the extreme value [45], was carried out. Among these factors, the most influential factors for EE and size were MT and TC, respectively (Table 3), which is consistent with the variance analysis (Table S1 and S2). The best levels for EE were $TC_2(CH/AL)_3MT_3$ (TC: 0.4%, CH/AL: 70:30, MT: 6 h), and the best combination for size was $TC_1(CH/AL)_1MT_1$ (TC: 0.08%, CH/AL: 20:80, MT: 0 h). Since the best combination of conditions for each EE ($TC_2(CH/AL)_3MT_3$) and size ($TC_1(CH/AL)_1MT_1$) were different, the linear weighted method with two weighting

Table 2. Orthogonal test design and results of CH-BSA-AL complexes

Factors	TC (%)	CH/AL (w/w)	MT (h)	EE (%)	Size (nm)
1	0.08	20:80	0	45.66 ± 4.51	329.13 ± 49.17
2	0.08	40:60	6	90.00 ± 1.11	688.67 ± 17.04
3	0.08	70:30	12	30.54 ± 0.41	581.83 ± 24.68
4	0.4	20:80	6	55.55 ± 4.99	1358.00 ± 612.28
5	0.4	40:60	12	57.63 ± 2.21	3251.73 ± 348.56
6	0.4	70:30	0	98.81 ± 1.43	5752.00 ± 587.74
7	0.8	20:80	12	62.37 ± 4.00	3022.67 ± 521.37
8	0.8	40:60	0	11.75 ± 3.60	774.97 ± 82.75
9	0.8	70:30	6	80.49 ± 33.79	8033.67 ± 814.14

TC: total concentration. CH/AL: ratio of chitosan and alginate. MT: mixing time. BSA: bovine serum albumin. EE: encapsulation efficiency.

Table 3. Encapsulation efficiency (EE) and size range analysis of orthogonal test of CH-BSA-AL complex

	TC (%)		CH/AL (w/w)		MT (h)	
	EE	Size	EE	Size	EE	Size
K1	166.19	1599.63	163.57	4709.80	156.22	6856.10
K2	211.99	10361.73	159.38	4715.37	226.04	10080.33
K3	154.61	11831.30	209.85	14367.50	150.54	6856.23
k1	55.40	533.21	54.52	1569.93	52.07	2285.37
k2	70.66	3453.91	53.13	1571.79	73.35	3360.11
k3	51.54	3943.77	69.95	4789.17	50.18	2285.41
The best level	TC_2	TC_1	$(CH/AL)_3$	$(CH/AL)_1$	MT_2	MT_1
Range	19.13	3410.56	16.82	3219.23	25.17	1074.74

Ki, the sum of test results corresponding to the level i on any column. Ki = Ki/3 (3, the amount of level).
TC: total concentration. CH/AL: ratio of chitosan and alginate. MT: mixing time. BSA: bovine serum albumin. EE: encapsulation efficiency.

coefficients (λ_1 and λ_2) [46] was applied to comprehensively consider the effect of three factors on both EE and size (Table S3). Depending on the importance of EE and size in the practical application, the weighted coefficient of EE (λ_1) is assigned 0.6, and size (λ_2) is assigned 0.4. The results showed that TC had the most influence on the formation of complex, which was followed by CH/AL. The most productive combination determined by the linear weighted analysis was $TC_1(CH/AL)_2MT_3$ (TC: 0.08%, CH/AL: 40:60, MT: 12 h).

To select the best condition from the above optimized groups, the complexes were prepared under three conditions, namely G1 (TC: 0.08%, CH/AL: 20:80, MT: 0 h), G2 (TC: 0.08%, CH/AL: 40:60, MT: 12 h), and G3 (TC: 0.4%, CH/AL: 70:30, MT: 6 h) (Table S4). G1 exhibited the smallest size (329.13 nm) with the lowest EE (45.66%). G2 exhibited the highest EE (96.3%) with the larger size (2,266 nm). The EE of G3 (81.0%) was lower than that of G2 but it exhibited the largest size (9,548 nm) (Table S4). Moreover, the PDI of G3 was over 0.9 (Table S5), indicating that the uniformity of this complex is too low to be utilized. Therefore, only G1 and G2 were used for further research.

3.2. Optimization of CH-BSA-AL complex formation process

3.2.1. Replacement of chitosan (CH) with low-molecular weight chitosan (LCH)

It is more desirable to reduce the size of G2 while retaining high EE. LCH has been widely used for the delivery of drugs or nutrients that require nanoparticle sizes and high bioavailability [47] with enhanced bioactivity, solubility, and biocompatibility [48,49]. Therefore, LCH replaces CH to encapsulate BSA when other factors and levels remain unchanged, namely LG1 and LG2. The sizes of LG1 (100.93 nm) and LG2 (957.8 nm) decreased and showed significant differences among the groups using CH (G1-LG1, p = 0.01; G2-LG2, p = 0.0498) in the case of negligible EE reduction (Table S6). Moreover, the PDI of LG1 reduced to 0.300 (Table S5). These results indicate that LCH reduces the size of complexes and improves their homogeneity compared with CH, therefore, LG1 and LG2 was used for further research.

3.2.2. Influence of embedding order on encapsulation and release

In the nanocomplex fabrication process, the cargo BSA was first complexed with AL. Since both BSA and AL are negatively charged in the reaction buffer, a repulsion force between them may hinder their complexation, which might lead to a low EE. Therefore, we firstly added LCH that was positively charged to the BSA rather than AL, namely LG3 and LG4. The EE of LG3 and LG4 significantly increased to 58.31% and 94.09% compared with LG1and LG2 ($p < 0.01$) (Table S6). Notably, the PDI of LG4 (0.308) was much lower than that of LG2 (0.649) (Table S5). These results indicate that the embedding LCH first in the complexation increases EE and homogeneity. In addition to the EE and size, the targeted and efficient release of the cargo BSA from complex is also a critical factor for evaluating a drug delivery ability. Therefore, the BSA release percentage of the four candidate complexes (LG1, LG2, LG3, and LG4) was further investigated.

3.3. pH-responsive bursting release of BSA

To verify the pH responsiveness of the complexes, the concentration of the BSA released from the complex in the supernatant was measured in pH 2.0 (0-2 h) and pH 7.4 (0-4 h) buffers at 37°C (Fig. 2). At pH 2.0, BSA was rarely released from all the four candidates for 2 h of incubation suggesting that the cargo protein was tightly encapsulated in response to the acidic environment mimicking a stomach. At pH 7.4, all the candidate complexes exhibited two release phases, the burst release phase (0-0.5 h) and the sustained release phase (1-4 h). The complexes from LG1 and LG4 released 29.96% and 12.70% of their cargo BSA

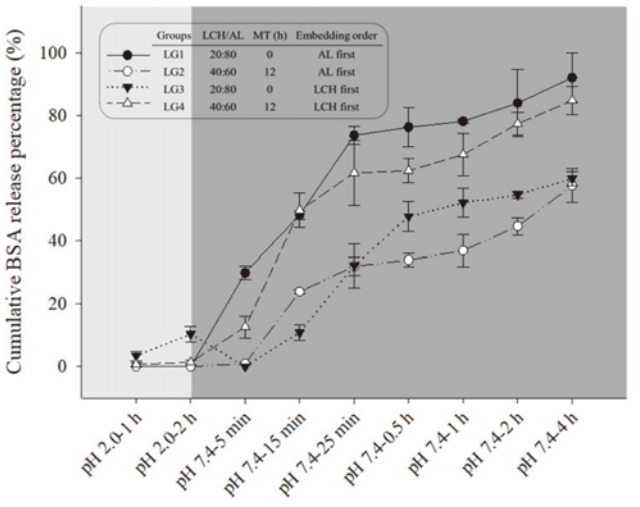

Fig. 2. Effect of LCH/AL, MT, and embedding order on BSA release percentage of the LCH-BSA-AL complexes at pH 2.0 and pH 7.4. The TC of LG1, LG2, LG3, and LG4 was 0.08%. LCH/AL: the ratio of low molecular chitosan and alginate (w/w). MT: mixing time. BSA: bovine serum albumin. TC: total concentration of chitosan and alginate.

protein for 5 min in the burst release phase, respectively, and the release ratio eventually increased to 76.31% and 61.74% for 25 min, respectively, which were much higher than those from LG2 and LG3 ($p < 0.01$) (Fig. 2). After the sustained release phase, LG1 eventually showed the highest BSA release (92.16%), and LG4 ranked the second highest percentage (84.87%) in the neutral pH condition mimicking an intestine. These release percentages were significantly higher than those of LG2 and LG3 ($p < 0.05$). To visualize the concentration of released BSA, the absolute amount was calculated according to the encapsulation efficiency (EE) of each candidate (Fig. S2). The absolute amount of BSA released from LG4 complex that eventually reached the small intestine was 78.78 μg/mL, which was significantly higher than that of other three candidate complexes ($p < 0.05$). The results indicate that these LCH-BSA-AL complexes pH-responsively encapsulate BSA at pH 2.0 and promote BSA release at pH 7.4.

The difference in release percentage among the four candidate complexes could be attributed to the embedding order that determines the dominant embedding mode of the BSA in the complexes. The isoelectric point (PI) of the BSA was 4.7. When the pH is above 4.7, the BSA is negatively charged; otherwise, it is positively charged. When the negatively charged AL solution (pH 6.33) was embedded first, the BSA (pH 6.70) was negative throughout the dropwise addition process. Thereafter, the CH-BSA-AL AL solution (pH 6.67) was added to the positively charged LCH solution (pH 2.90) dropwise. During this period, the negatively charged BSA would gradually become positive owing to the lower pH than its PI. The BSA is more likely to bind to the AL with negative charge rather than the LCH with a positive charge in the final polyelectrolyte complex solution (Fig. S3A), resulting in an AL-dominated embedding mode. However, when the positively charged LCH solution (pH 2.90) was embedded first, the negatively charged BSA (pH 6.70) gradually became positively charged during the addition process. Thereafter, the CH-BSA-AL LCH solution (pH 3.16) was added to the AL dropwise. During this period, the positive charge of the BSA would gradually become negative owing to the higher pH than its PI. The BSA is more likely to bind to the positively charged LCH rather than the negatively charged AL in the final polyelectrolyte complex solution (Fig. S3B), resulting in an LCH-dominated embedding mode.

On the other hand, the AL structure is rich in hydroxyl groups, whereas the LCH structure is rich in amino groups and has only a small amount of hydroxyl groups [26]. The presence of hydroxyl and amino groups causes a structural swelling at high and low pH conditions, respectively [50]. When AL was embedded first (LG1 and LG2), the candidate with the higher proportion of AL (LG1) increased the BSA release percentage. In the same way, the candidate with the higher proportion of LCH (LG4) boosted the BSA release when the LCH was embedded first (LG3 and LG4). Furthermore, the complexes fabricated through the LCH-dominated embedding mode exhibited higher release (LG3: 10.42%, LG4: 1.35%) at pH 2.0 than those of LG1 and LG2 through the AL-dominated embedding mode.

3.4. Characterization of pH-responsive CH-BSA-AL complexes

3.4.1. Size and ζ-potential of pH-responsive CH-BSA-AL complexes

To figure out the probable cause of the difference in release percentage between pH 2.0 and 7.4, the change in the complex size and ζ-potential was continuously monitored (Fig. 3A and 3B). After 2 h of incubation at pH 2.0, the sizes of complexes from LG1, LG2, LG3, and LG4 were 11,532, 4,785, 3,195, and 8,994 nm, respectively. These candidates presented significantly smaller sizes when those complexes were immersed in the pH 7.4 buffer during the first 0.5 h (LG1: 1,901 nm, LG2: 483 nm, LG3: 465 nm, and LG4: 2,492 nm). After 4 h, larger sizes were observed in LG1 (2,703 nm) and LG4 (1,649 nm) in comparison with those of LG2 (738 nm) and LG3 (311 nm) (Fig. 3A). The size of complex will increase with swelling of AL in a moderately alkaline environment. The larger sizes of complexes from LG1 and LG4 was presumably because they were more swollen than the other candidates, LG2

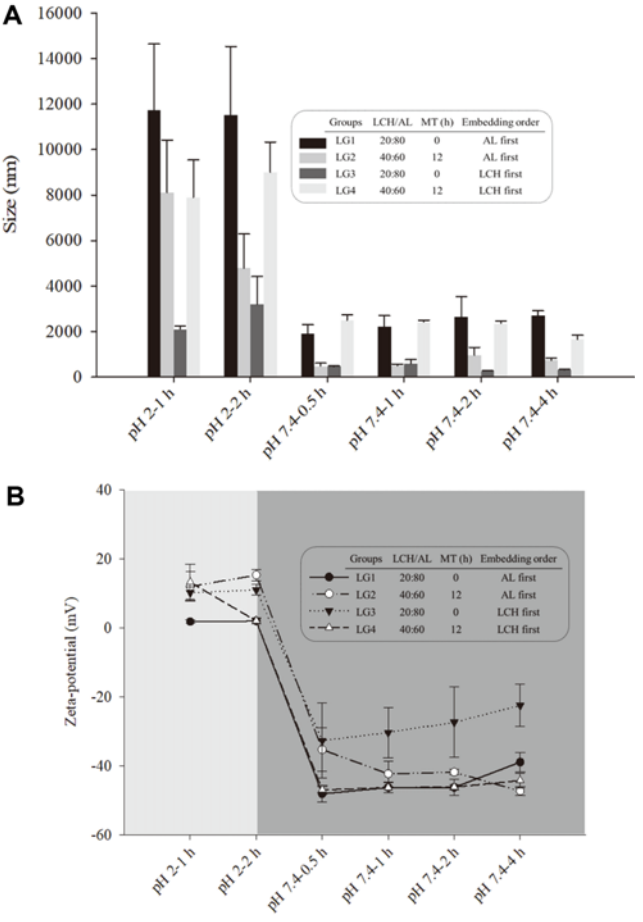

Fig. 3. Effect of LCH/AL, MT, and embedding order on size (A) and ζ-potential (B) of the LCH-BSA-AL complexes at pH 2.0 and pH 7.4. The TC of LG1, LG2, LG3, and LG4 was 0.08% (w/w). LCH/AL: the ratio of low molecular chitosan and alginate (w/w). BSA: bovine serum albumin. MT: mixing time. TC: total concentration of chitosan and alginate.

and LG3. The higher the degree of swelling (*DS*) allows the BSA to be released more easily from the complexes. Therefore, the BSA release percentages for complexes from LG1 and LG4 at pH 7.4 were higher than those for complexes from LG2 and LG3 (Fig. 2).

However, the large size of complexes at pH 2.0 was not because of the swelling but due to the particle-particle aggregation, which was supported by the ζ-potential results. The absolute ζ-potential values of the complexes at pH 2.0 from LG1, LG2, LG3, and LG4 were 1.91, 15.23, 10.94, and 1.98 mV, respectively. The absolute ζ-potentials for all candidates at pH 7.4 increased up to 48.17, 47, 35.37, and 32.77 mV in LG1, LG2, LG3, and LG4, respectively at 0.5 h (Fig. 3B). The instabilities of complexes are mainly attributed to the accumulation of migrating or diffusing particles, which can be hindered by high surface charges or electric potentials. When the absolute ζ-potential is between 10 and 20, it indicates that the particles are unstable, and they tend to aggregate. When the value is between 0 and 5, it indicates that the particles aggregate rapidly [51]. The large size exhibited at pH 2.0 was more likely to be caused by the aggregation of single particles rather than complex swelling, suggesting that all the candidates were pH-responsive (pH 2.0-7.4). In addition, the aggregated complexes were able to disaggregate and form small single particles under neutral pH condition, which was independent of the previous acid aggregation.

3.4.2. Morphology of pH-responsive CH-BSA-AL complex

To examine the morphological changes of complexes with their pH-responsiveness, the best candidate (LG4) was observed using a scanning electron microscope (SEM). In previous studies, most complexes comprising AL and CH as vehicles were fabricated using cross-linkers to facilitate complex formation [52-54]. However, the cross-linkers caused a delayed release (Fig. S4), which was opposite to our objective of a bursting release of cargo molecules. The SEM images showed that the CH-BSA-AL complexes were successfully constructed without cross-linkers (Fig. 4A). The shape of LCH-BSA-AL complexes was a spherical-like polyhedron with several angles. In a previous study, a similar spherical CH-AL nanoparticle loaded with rutin was constructed using $CaCl_2$ as a cross-linker [55]. An aggregation of individual particles was observed when

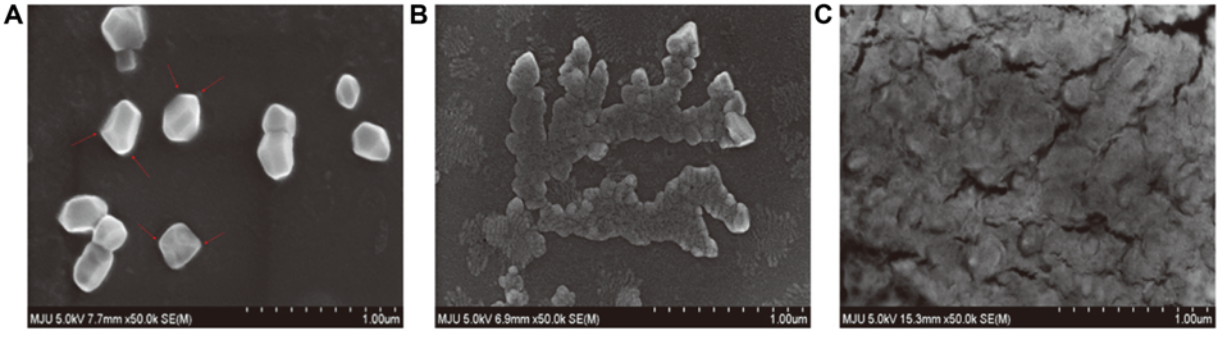

Fig. 4. Scanning electron microscopy (SEM) image of LCH-BSA-AL complex from LG4 process (A) and the complex at pH 2.0 after 2 h (B) and at pH 7.4 after 4 h (C) of incubation. LCH: low molecular chitosan. BSA: bovine serum albumin. AL: alginate.

complexes were immersed in the pH 2.0 buffer for 2 h (Fig. 4B). However, neither the individual nor aggregated complexes were observed after 4 h of incubation in the pH 7.4 buffer, suggesting an amorphous disruption of particulates (Fig. 4C). The complex-complex aggregation at pH 2.0 resulted in large size particulates (> 1,000 nm) (Fig. 3A) and low absolute values of ζ-potential (0-20 mV) (Fig. 3B). Such aggregation led to the sufficient encapsulation and rare release of cargo protein at pH 2.0. Upon a change of environmental pH from 2.0 to 7.4, the aggregates of complexes were disrupted, and the particulate complex of LCH-BSA-AL were subsequently or previously burst within the short period (0.5 h). The amorphous powders observed cargo protein BSA into the solution.

3.5. Macroscale swelling of CH-BSA-AL complex

A disruption of aggregated complexes was observed in micro- or nanoscale environment at pH 7.4, which was

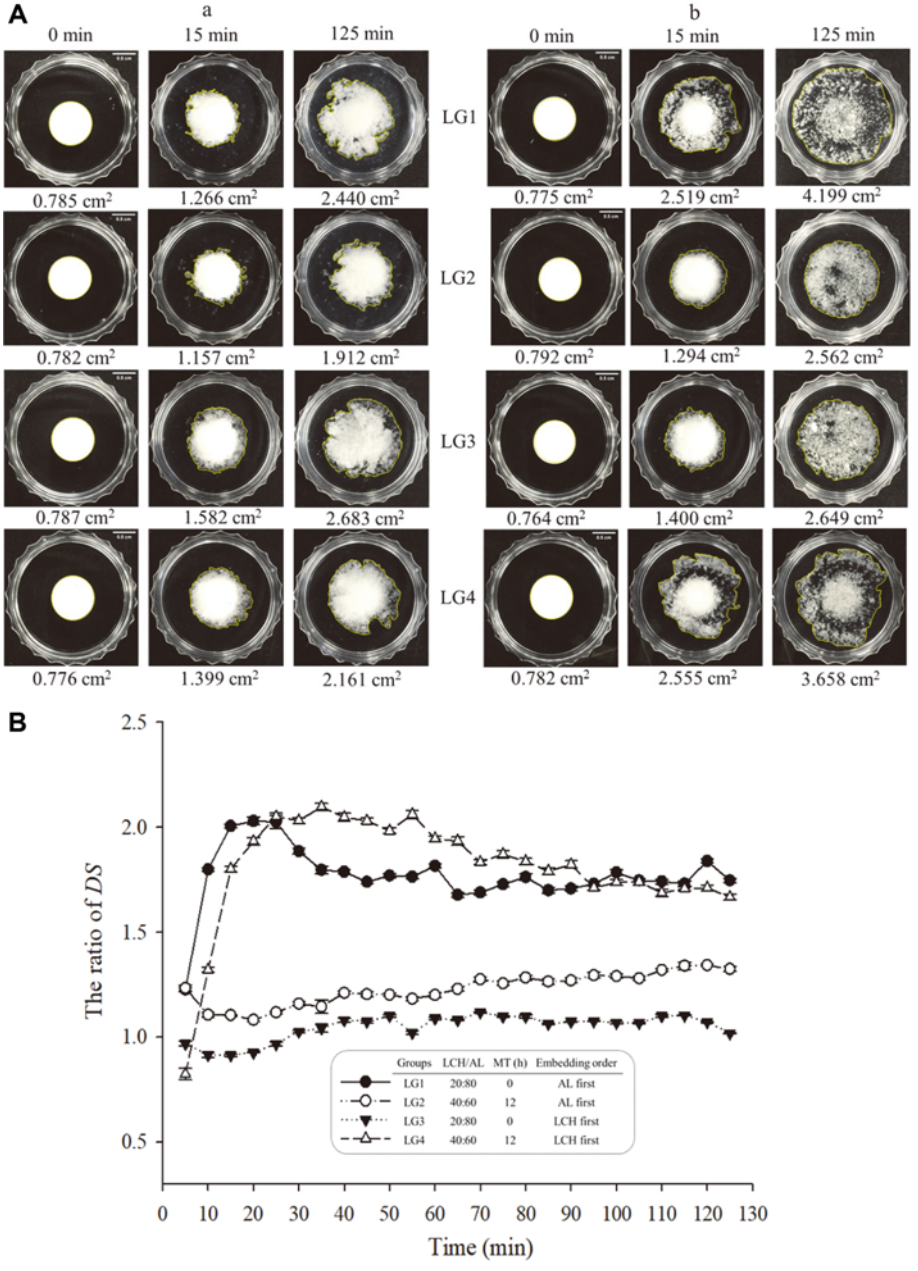

Fig. 5. (A) Dried and swollen tablets at pH 2.0 (a) and pH 7.4 (b) at the indicated time points. The number below each photo represents the area of the tablet at the indicated time points. Scale bar: 0.5 cm. (B) Effect of LCH/AL, MT, and embedding order on the ratio of degree of swelling (*DS*) of the CH-BSA-AL complex in pH 2.0 to pH 7.4 buffer. The TC of LG1, LG2, LG3, and LG4 was 0.08% (w/w). LCH/AL: the ratio of low molecular chitosan and alginate (w/w). BSA: bovine serum albumin. TC: total concentration.

supported by SEM images, sizes and ζ-potentials. To determine whether this disruption occurs in the macroscopic environment, we examined degree of swelling (*DS*) of tablets which were made of CH-BSA-AL complexes (Fig. 5). The *DS* of tablets made of LG1, LG2, and LG4 complexes was faster and higher in pH 7.4 (Fig. 5Aa) than pH 2.0 (Fig. 5Ab), suggesting that the micro- or nanoscale particle disruption led to the macroscale disruption. During the 125 min, the ratio of *DS* for LG1, LG2, and LG4 were greater than 1, whereas that of LG3 fluctuated to slightly around 1 (Fig. 5B), which indicated that the *DS* of LG1, LG2, and LG4 in pH 7.4 were greater than that in pH 2.0. During the first 25 min, the ratio of *DS* of LG1 and LG4 increased rapidly to their maximum values, which were 2.03 and 2.05, respectively. These values were significantly higher in comparison with those of LG2 (1.12) and LG3 (0.97) ($p < 0.05$). At 125 min, the ratio of *DS* increased in the order: LG1 > LG4 > LG2 > LG3, which exactly corresponds to the result of BSA release percentages (Fig. 2). A similar result was also demonstrated in the previous study by Khan *et al.* [50]. The samples with high concentrations of polyvinyl alcohol (PVA) as a coating material exhibited a higher drug release due to the high swelling ratio, which was directly proportional to the PVA contents.

4. Conclusion

In this study, a pH-responsive complex with bursting release consisting of low molecular chitosan (LCH) and alginate (AL) was successfully fabricated without cross-linkers. The variance analysis of the orthogonal test showed that total concentration (TC) was the critical factor determining encapsulation efficiency (EE) and complex size. Through the orthogonal test and further optimization, four candidate complexes were obtained (LG1, LG2, LG3, and LG4) and their BSA release percentage, physicochemical characteristics, and degree of swelling (*DS*) were investigated to find an optimized fabrication process. SEM images indicate that a spherical-like polyhedron with several angels was successfully constructed. LG4 is the optimized candidate due to the highest effective dose (78.78 mg/mL) caused by high EE at pH 2.0 and large release percentage at pH 7.4. The enhanced release percentages of BSA led to the enlarged ratio of degree of swelling (*DS*) from LG1 and LG4 complexes at pH 7.4. The cross-linker-free and pH-responsive LCH-BSA-AL complex has a great potential for protein drug or vaccine delivery by its aggregation at stomach (pH 2.0) and bursting release at intestinal tract (pH 7.4).

Acknowledgements

This research was funded by National Research Foundation (NRF, 2021R1A2C1004626) and Cooperative Research Program for Agriculture Science and Technology Development (PJ01320502) of Rural Development Administration, Republic of Korea.

Conflict of Interest

The authors have no conflict of interest to declare.

Ethical Statement

Neither ethical approval nor informed consent was required for this study.

Electronic Supplementary Material (ESM)

The online version of this article (doi: 10.1007/s12257-021-0243-6) contains supplementary material, which is available to authorized users.

Nomenclature

Nomenclature	Wall materials	CH/AL (w/w)	MT (h)	Embedding order
G1	AL and CH	20:80	0	AL first
G2	AL and CH	40:60	12	AL first
G3	AL and CH	70:30	6	AL first
LG1	AL and LCH	20:80	0	AL first
LG2	AL and LCH	40:60	12	AL first
LG3	AL and LCH	20:80	0	LCH first
LG4	AL and LCH	40:60	12	LCH first

Abbreviations	Definition
AL	Alginate
BSA	Bovine serum albumin
CH	Chitosan
CH/AL	Ratio of CH and AL (w/w)
DS	Degree of swelling
EE	Encapsulation efficiency
GI	Gastrointestinal
LCH	Low molecular chitosan
MT	Mixing time
PBS	Phosphatic buffer solution

PDI	Polymer disperse index
PI	Isoelectric point
SEM	Scanning Electron Microscope
TC	Total concentration of CH and AL

References

1. Usmani, S. S., G. Bedi, J. S. Samuel, S. Singh, S. Kalra, P. Kumar, A. A. Ahuja, M. Sharma, A. Gautam, and G. P. S. Raghava (2017) THPdb: Database of FDA-approved peptide and protein therapeutics. *PLoS One.* 12: e0181748.
2. Lagassé, H. A. D., A. Alexaki, V. L. Simhadri, N. H. Katagiri, W. Jankowski, Z. E. Sauna, and C. Kimchi-Sarfaty (2017) Recent advances in (therapeutic protein) drug development. *F1000Res*. 6: 113.
3. Pawar, R., A. Ben-Ari, and A. J. Domb (2004) Protein and peptide parenteral controlled delivery. *Expert Opin. Biol. Ther.* 4: 1203-1212.
4. Shone, A., J. Burnside, S. Chipchase, F. Game, and W. Jeffcoate (2006) Probing the validity of the probe-to-bone test in the diagnosis of osteomyelitis of the foot in diabetes. *Diabetes Care*. 29: 945.
5. Messer, L. H., C. Berget, C. Beatson, S. Polsky, and G. P. Forlenza (2018) Preserving skin integrity with chronic device use in diabetes. *Diabetes Technol. Ther*. 20: S254-S264.
6. Richardson, T. and D. Kerr (2003) Skin-related complications of insulin therapy: Epidemiology and emerging management strategies. *Am. J. Clin. Dermatol.* 4: 661-667.
7. Kerbleski, J. F. and A. B. Gottlieb (2009) Dermatological complications and safety of anti-TNF treatments. *Gut.* 58: 1033-1039.
8. Yoshida, M., N. Kamei, K. Muto, J. Kunisawa, K. Takayama, N. A. Peppas, and M. Takeda-Morishita (2017) Complexation hydrogels as potential carriers in oral vaccine delivery systems. *Eur. J. Pharm. Biopharm.* 112: 138-142.
9. Biswas, S., M. Chattopadhyay, K. K. Sen, and M. K. Saha (2015) Development and characterization of alginate coated low molecular weight chitosan nanoparticles as new carriers for oral vaccine delivery in mice. *Carbohydr. Polym.* 121: 403-410.
10. Marasini, N., M. Skwarczynski, and I. Toth (2014) Oral delivery of nanoparticle-based vaccines. *Expert Rev. Vaccines.* 13: 1361-1376.
11. Zhou, X. and A. L. W. Po (1991) Peptide and protein drugs: II. Non-parenteral routes of delivery. *Int. J. Pharm.* 75: 117-130.
12. Fjellestad-Paulsen, A., P. Höglund, S. Lundin, and O. Paulsen (1993) Pharmacokinetics of 1-deamino-8-D-arginine vasopressin after various routes of administration in healthy volunteers. *Clin. Endocrinol.* 38: 177-182.
13. Brown, T. D., K. A. Whitehead, and S. Mitragotri (2020) Materials for oral delivery of proteins and peptides. *Nat. Rev. Mater.* 5: 127-148.
14. Villa, L. L., R. L. R. Costa, C. A. Petta, R. P. Andrade, K. A. Ault, A. R. Giuliano, C. M. Wheeler, L. A. Koutsky, C. Malm, M. Lehtinen, F. E. Skjeldestad, S. E. Olsson, M. Steinwall, D. R. Brown, R. J. Kurman, B. M. Ronnett, M. H. Stoler, A. Ferenczy, D. M. Harper, G. M. Tamms, J. Yu, L. Lupinacci, R. Railkar, F. J. Taddeo, K. U. Jansen, M. T. Esser, H. L. Sings, A. J. Saah, and E. Barr (2005) Prophylactic quadrivalent human papillomavirus (types 6, 11, 16, and 18) L1 virus-like particle vaccine in young women: a randomised double-blind placebo-controlled multicentre phase II efficacy trial. *Lancet Oncol.* 6: 271-278.
15. Giannini, S. L., E. Hanon, P. Moris, M. Van Mechelen, S. Morel, F. Dessy, M. A. Fourneau, B. Colau, J. Suzich, G. Losonksy, M. T. Martin, G. Dubin, and M. A. Wettendorff (2006) Enhanced humoral and memory B cellular immunity using HPV16/18 L1 VLP vaccine formulated with the MPL/aluminium salt combination (AS04) compared to aluminium salt only. *Vaccine.* 24: 5937-5949.
16. Slupetzky, K., R. Gambhira, T. D. Culp, S. Shafti-Keramat, C. Schellenbacher, N. D. Christensen, R. B. S. Roden, and R. Kirnbauer (2007) A papillomavirus-like particle (VLP) vaccine displaying HPV16 L2 epitopes induces cross-neutralizing antibodies to HPV11. *Vaccine*. 25: 2001-2010.
17. Baca-Estrada, M. E., M. Foldvari, M. Snider, K. Harding, B. Kournikakis, L. A. Babiuk, and P. Griebel (2000) Intranasal immunization with liposome-formulated *Yersinia pestis* vaccine enhances mucosal immune responses. *Vaccine.* 18: 2203-2211.
18. Karkada, M., G. M. Weir, T. Quinton, A. Fuentes-Ortega, and M. Mansour (2010) A liposome-based platform, VacciMax®, and its modified water-free platform DepoVax™ enhance efficacy of *in vivo* nucleic acid delivery. *Vaccine.* 28: 6176-6182.
19. Demento, S. L., W. Cui, J. M. Criscione, E. Stern, J. Tulipan, S. M. Kaech, and T. M. Fahmy (2012) Role of sustained antigen release from nanoparticle vaccines in shaping the T cell memory phenotype. *Biomaterials*. 33: 4957-4964.
20. Dhar, S., W. L. Daniel, D. A. Giljohann, C. A. Mirkin, and S. J. Lippard (2009) Polyvalent oligonucleotide gold nanoparticle conjugates as delivery vehicles for platinum (IV) warheads. *J. Am. Chem. Soc.* 131: 14652-14653.
21. Elzoghby, A. O., W. M. Samy, and N. A. Elgindy (2012) Albumin-based nanoparticles as potential controlled release drug delivery systems. *J. Control. Release.* 157: 168-182.
22. Muzzarelli, R. A. (1997) Human enzymatic activities related to the therapeutic administration of chitin derivatives. *Cell. Mol. Life Sci.* 53: 131-140.
23. Shimoda, J., H. Onishi, and Y. Machida (2001) Bioadhesive characteristics of chitosan microspheres to the mucosa of rat small intestine. *Drug Dev. Ind. Pharm.* 27: 567-576.
24. Sahoo, P., K. H. Leong, S. Nyamathulla, Y. Onuki, K. Takayama, and L. Y. Chung (2019) Chitosan complexed carboxymethylated *iota*-carrageenan oral insulin particles: Stability, permeability and *in vivo* evaluation. *Mater. Today Commun*. 20: 100557.
25. Remuñán-López, C., A. Portero, J. L. Vila-Jato, and M. J. Alonso (1998) Design and evaluation of chitosan/ethylcellulose mucoadhesive bilayered devices for buccal drug delivery. *J. Control. Release.* 55: 143-152.
26. George, M. and T. E. Abraham (2006) Polyionic hydrocolloids for the intestinal delivery of protein drugs: alginate and chitosan—a review. *J. Control. Release.* 114: 1-14.
27. Orive, G., S. Ponce, R. M. Hernandez, A. R. Gascon, M. Igartua, and J. L. Pedraz (2002) Biocompatibility of microcapsules for cell immobilization elaborated with different type of alginates. *Biomaterials.* 23: 3825-3831.
28. Li, R., P. De Bank, and R. Mrsny (2016) Increase alginate-chitosan nanoparticles transport efficiency through the epithelium by attaching nt-PE onto surface. *Proceedings of the World Congress on Recent Advances in Nanotechnology*. April 1-2. Prague, Czech Republic.
29. Chen, S. C., Y. C. Wu, F. L. Mi, Y. H. Lin, L. C. Yu, and H. W. Sung (2004) A novel pH-sensitive hydrogel composed of N,O-carboxymethyl chitosan and alginate cross-linked by genipin for protein drug delivery. *J. Control. Release.* 96: 285-300.
30. Banks, S. R., K. Enck, M. Wright, E. C. Opara, and M. E. Welker (2019) Chemical modification of alginate for controlled oral drug delivery. *J. Agric. Food Chem.* 67: 10481-10488.
31. Cikrikci, S., B. Mert, and M. H. Oztop (2018) Development of pH sensitive alginate/gum tragacanth based hydrogels for oral insulin delivery. *J. Agric. Food Chem.* 66: 11784-11796.

32. Wu, T., S. Yu, D. Lin, Z. Wu, J. Xu, J. Zhang, Z. Ding, Y. Miao, T. Liu, T. Chen, and X. Cai (2020) Preparation, characterization, and release behavior of doxorubicin hydrochloride from dual cross-linked chitosan/alginate hydrogel beads. *ACS Appl. Bio Mater.* 3: 3057-3065.
33. Khajuria, D. K., R. Vasireddi, M. K. Priydarshi, and D. R. Mahapatra (2020) Ionic diffusion and drug release behavior of core-shell-functionalized alginate-chitosan-based hydrogel. *ACS Omega.* 5: 758-765.
34. Damera, D. P., S. Kaja, L. S. L. Janardhanam, S. Alim, V. V. K. Venuganti, and A. Nag (2019) Synthesis, detailed characterization, and dual drug delivery application of BSA loaded aquasomes. *ACS Appl. Bio Mater.* 2: 4471-4484.
35. Damera, J., L. Schorn, A. Landers, H. Holtmann, K. Berr, N. R. Kübler, C. Sproll, M. Rana, and R. Depprich (2019) Release kinetics of the model protein FITC-BSA from different polymer-coated bovine bone substitutes. *Head Face Med.* 15: 27.
36. Jing, Z. W., Z. W. Ma, C. Li, Y. Y. Jia, M. Luo, X. X. Ma, S. Y. Zhou, and B. L. Zhang (2017) Chitosan cross-linked with poly(ethylene glycol)dialdehyde via reductive amination as effective controlled release carriers for oral protein drug delivery. *Bioorg. Med. Chem. Lett.* 27: 1003-1006.
37. Xu, Y., L. An, L. Chen, H. Xu, D. Zeng, and G. Wang (2018) Controlled hydrothermal synthesis of strontium-substituted hydroxyapatite nanorods and their application as a drug carrier for proteins. *Adv. Powder Technol.* 29: 1042-1048.
38. Takka, S. and A. Gürel (2020) Evaluation of chitosan/alginate beads using experimental design: formulation and *in vitro* characterization. *AAPS PharmSciTech.* 11: 460-466.
39. Tapia, C., E. Costa, M. Moris, J. Sapag-Hagar, F. Valenzuela, and C. Basualto (2002) Study of the influence of the pH media dissolution, degree of polymerization, and degree of swelling of the polymers on the mechanism of release of diltiazem from matrices based on mixtures of chitosan/alginate. *Drug Dev. Ind. Pharm.* 28: 217-224.
40. Cheng, L., C. Bulmer, and A. Margaritis (2015) Characterization of novel composite alginate chitosan-carrageenan nanoparticles for encapsulation of BSA as a model drug delivery system. *Curr. Drug Deliv.* 12: 351-357.
41. Krieg, R. C., Y. Dong, K. Schwamborn, and R. Knuechel (2005) Protein quantification and its tolerance for different interfering reagents using the BCA-method with regard to 2D SDS PAGE. *J. Biochem. Biophys. Methods.* 65: 13-19.
42. Li, X., X. Kong, S. Shi, X. Zheng, G. Guo, Y. Wei, and Z. Qian (2008) Preparation of alginate coated chitosan microparticles for vaccine delivery. *BMC Biotechnol.* 8: 89.
43. Yu, C. Y., B. C. Yin, W. Zhang, S. X. Cheng, X. Z. Zhang, and R. X. Zhuo (2009) Composite microparticle drug delivery systems based on chitosan, alginate and pectin with improved pH-sensitive drug release property. *Colloids Surf. B. Biointerfaces.* 68: 245-249.
44. Chen, B., W. Kong, N. Wang, G. Zhu, and F. Wang (2019) Oleylamine-mediated synthesis of small NaYbF4 nanoparticles with tunable size. *Chem. Mater.* 31: 4779-4786.
45. Gao, X., Y. Zhang, H. Zhang, and Q. Wu (2012) Effects of machine tool configuration on its dynamics based on orthogonal experiment method. *Chin. J. Aeronaut.* 25: 285-291.
46. Yeh, C. H., M. H. Lin, P. C. Chang, and L. W. Kang (2020) Enhanced visual attention-guided deep neural networks for image classification. *IEEE Access*. 8: 163447-163457.
47. Arunkumar, R., K. V. H. Prashanth, and V. Baskaran (2013) Promising interaction between nanoencapsulated lutein with low molecular weight chitosan: Characterization and bioavailability of lutein *in vitro* and *in vivo*. *Food Chem.* 141: 327-337.
48. Lee, M., J. W. Nah, Y. Kwon, J. J. Koh, K. S. Ko, and S. W. Kim (2001) Water-soluble and low molecular weight chitosan-based plasmid DNA delivery. *Pharm. Res.* 18: 427-431.
49. Chae, S. Y., M. K. Jang, and J. W. Nah (2005) Influence of molecular weight on oral absorption of water soluble chitosans. *J. Control. Release.* 102: 383-394.
50. Khan, S. and N. M. Ranjha (2014) Effect of degree of cross-linking on swelling and on drug release of low viscous chitosan/poly(vinyl alcohol) hydrogels. *Polym. Bull.* 71: 2133-2158.
51. Marín, R. R. R., F. Babick, and L. Hillemann (2017) Zeta potential measurements for non-spherical colloidal particles-practical issues of characterisation of interfacial properties of nanoparticles. *Colloids Surf. A. Physicochem. Eng. Asp.* 532: 516-521.
52. Caetano, L. A., A. J. Almeida, and L. M. D. Gonçalves (2016) Effect of experimental parameters on alginate/chitosan microparticles for BCG encapsulation. *Mar. Drugs.* 14: 90.
53. Dudek, G. and R. Turczyn (2018) New type of alginate/chitosan microparticle membranes for highly efficient pervaporative dehydration of ethanol. *RSC Adv.* 8: 39567-39578.
54. Lakkakula, J. R., T. Matshaya, and R. W. M. Krause (2017) Cationic cyclodextrin/alginate chitosan nanoflowers as 5-fluorouracil drug delivery system. *Mater. Sci. Eng. C. Mater. Biol. Appl.* 70: 169-177.
55. Mujtaba, M. A., K. A. M. Hassan, and M. Imran (2018) Chitosan-alginate nanoparticles as a novel drug delivery system for rutin. *Int. J. Adv. Biotechnol. Res.* 9: 1895-903.